

# A LEVEL-2 TRIGGER ALGORITHM FOR THE IDENTIFICATION OF MUONS IN THE ATLAS MUON SPECTROMETER

A. Di Mattia on behalf of the ATLAS HLT group \*

## Abstract

The ATLAS Level-2 trigger provides a software-based event selection after the initial Level-1 hardware trigger. For the muon events, the selection is decomposed in a number of broad steps: first, the Muon Spectrometer data are processed to give physics quantities associated to the muon track (standalone feature extraction) then, other detector data are used to refine the extracted features. The “ $\mu$ Fast” algorithm performs the standalone feature extraction, providing a first reduction of the muon event

rate from Level-1. It confirms muon track candidates with a precise measurement of the muon momentum. The algorithm is designed to be both conceptually simple and fast so as to be readily implemented in the demanding online environment in which the Level-2 selection code will run. Nevertheless its physics performance approaches, in some cases, that of the offline reconstruction algorithms. This paper describes the implemented algorithm together with the software techniques employed to increase its timing performances.

## INTRODUCTION

The ATLAS experiment [1] will search new particles at the Large Hadron Collider (LHC), the CERN p-p ring designed to provide 14 TeV centre of mass energy and  $10^{34}\text{cm}^{-2}\text{s}^{-1}$  maximum luminosity. These values of energy and luminosity will allow to probe the High Energy Physics frontier up to the scale of  $\sim 1$  TeV but will also set an harsh experimental environment where the QCD background particles have a production rate several orders of magnitude greater than the physics signals.

Moreover, the high particle flux and the short bunch crossing separation, 25 ns, impose to use fast time response detectors with a fine read-out granularity, especially for the central tracker. This implies a large number of electronics channels that produce a very large amount of data ( $O(10^8)$  MByte/s).

Therefore triggering at LHC will be more difficult than in current experiments: the huge event rate,  $O(1\text{GHz})$ , must be reduced to a manageable level (10-100 events/s) for the storage system and the offline computing. The trigger must provide an event rejection of  $10^7$  and, in order to cope with the high QCD background, it must be able to identify physics objects with performances similar to the offline selection.

Among the several trigger subsystems the one based on muon identification and reconstruction is particularly important because it allows the selection of the cleanest channel for the Higgs discovery ( $H \rightarrow ZZ \rightarrow 4\mu$ ) and of events for precision physics (CP violation,  $M_W$ ).

## THE ATLAS MUON SYSTEM

The ATLAS Muon System [2] is designed to provide muon identification and to perform a standalone high precision measurement of the muon momentum up to  $\eta \approx 3$ . It exploits three air core toroidal magnets providing a field of 0.5 Tesla. Inside the magnetic field are housed

\* S. Armstrong<sup>a</sup>, A. dos Anjos<sup>b</sup>, J.T.M. Baines<sup>c</sup>, C.P. Bee<sup>d</sup>, M. Biglietti<sup>e</sup>, J.A. Bogaerts<sup>f</sup>, V. Boisvert<sup>f</sup>, M. Bosman<sup>g</sup>, B. Caron<sup>h</sup>, P. Casado<sup>g</sup>, G. Cataldi<sup>i</sup>, D. Cavalli<sup>j</sup>, M. Cervetto<sup>k</sup>, G. Comune<sup>l</sup>, P. Conde Muino<sup>l</sup>, A. De Santo<sup>m</sup>, A. Di Mattia<sup>n</sup>, M. Diaz Gomez<sup>o</sup>, M. Dosit<sup>g</sup>, N. Ellis<sup>f</sup>, D. Emeliyanov<sup>g</sup>, B. Epp<sup>p</sup>, S. Falciano<sup>n</sup>, A. Farilla<sup>q</sup>, S. George<sup>m</sup>, V. Ghete<sup>p</sup>, S. González<sup>r</sup>, M. Grothe<sup>f</sup>, S. Kabana<sup>l</sup>, A. Khomich<sup>s</sup>, G. Kilvington<sup>m</sup>, N. Kostantinidis<sup>l</sup>, A. Kootz<sup>q</sup>, A. Lowe<sup>m</sup>, C. Luci<sup>n</sup>, L. Luminari<sup>n</sup>, T. Maeno<sup>l</sup>, F. Marzano<sup>n</sup>, J. Masik<sup>v</sup>, C. Meessen<sup>d</sup>, A.G. Mello<sup>b</sup>, G. Merino<sup>g</sup>, R. Moore<sup>h</sup>, P. Morettini<sup>k</sup>, A. Negri<sup>w</sup>, N. Nikitin<sup>x</sup>, A. Nisati<sup>n</sup>, C. Padilla<sup>f</sup>, N. Panikashvili<sup>y</sup>, F. Parodi<sup>k</sup>, E. Pasqualucci<sup>q</sup>, V. Perez Reale<sup>l</sup>, J.L. Pinfold<sup>h</sup>, P. Pinto<sup>f</sup>, Z. Qian<sup>d</sup>, S. Resconi<sup>r</sup>, S. Rosati<sup>f</sup>, C. Sanchez<sup>g</sup>, C. Santamarina<sup>f</sup>, D.A. Scannicchio<sup>w</sup>, C. Schiavi<sup>k</sup>, E. Segura<sup>g</sup>, J.M. de Seixas<sup>b</sup>, S. Sivoklokov<sup>x</sup>, R. Soluk<sup>h</sup>, E. Stefanidis<sup>l</sup>, S. Sushkov<sup>g</sup>, M. Sutton<sup>l</sup>, S. Tapprogge<sup>z</sup>, E. Thomas<sup>l</sup>, F. Touchard<sup>d</sup>, B. Venda Pinto<sup>aa</sup>, V. Vercesi<sup>w</sup>, P. Werner<sup>f</sup>, S. Wheeler<sup>h,bb</sup>, F.J. Wickens<sup>c</sup>, W. Wiedenmann<sup>f</sup>, M. Wielers<sup>cc</sup>, G. Zoernig<sup>f</sup>.

<sup>a</sup>Brookhaven National Laboratory (BNL), Upton, New York, USA,

<sup>b</sup>Universidade Federal do Rio de Janeiro, COPPE/EE, Rio de Janeiro,

Barzil. <sup>c</sup>Rutherford Appleton Laboratory, Chilton, Didcot, UK, <sup>d</sup>Centre

de Physique des Particules de Marseille, IN2P3-CNRS-Université d'Aix-

Marseille 2, France, <sup>e</sup>University of Michigan, Ann Arbor, Michigan,

USA, <sup>f</sup>CERN, Geneva, Switzerland, <sup>g</sup>Institut de Física d'Altes Energies

(IFAE), Universidad Autónoma de Barcelona, Barcelona, Spain,

<sup>h</sup>University of Alberta, Edmonton, Canada, <sup>i</sup>Dipartimento di Fisica

dell'Università di Lecce e I.N.F.N., Lecce, Italy, <sup>j</sup>Dipartimento di Fisica

dell'Università di Milano e I.N.F.N., Milan, Italy, <sup>k</sup>Dipartimento di

Fisica dell'Università di Genova e I.N.F.N., Genoa, Italy, <sup>l</sup>Laboratory

for High Energy Physics, University of Bern, Switzerland, <sup>m</sup>Department

of Physics, Royal Holloway, University of London, Egham, UK,

<sup>n</sup>Dipartimento di Fisica dell'Università di Roma 'La Sapienza' e

I.N.F.N., Rome, Italy, <sup>o</sup>Section de Physique, Université de Genève,

Switzerland, <sup>p</sup>Institut für Experimentalphysik der Leopold-Franzens

Universität, Innsbruck, Austria, <sup>q</sup>Dipartimento di Fisica dell'Università

di Roma 'Roma Tre' e I.N.F.N., Rome, Italy, <sup>r</sup>Department of Physics,

University of Wisconsin, Madison, Wisconsin, USA, <sup>s</sup>Lehrstuhl für

Informatik V, Universität Mannheim, Mannheim, Germany, <sup>t</sup>Department

of Physics and Astronomy, University College London, London, UK,

<sup>u</sup>Fachbereich Physik, Bergische Universität Wuppertal, Germany,

<sup>v</sup>Institute of Physics, Academy of Sciences of the Czech Republic,

Prague, Czech Republic, <sup>w</sup>Dipartimento di Fisica Nucleare e Teorica

dell'Università di Pavia e I.N.F.N., Pavia, Italy, <sup>x</sup>Institute of Nuclear

Physics, Moscow State University, Moscow, Russia, <sup>y</sup>Department of

Physics, Technion, Haifa, Israel, <sup>z</sup>Institut für Physik, Universität Mainz,

Mainz, Germany, <sup>aa</sup>CFNUL – Universidade de Lisboa, Faculdade de

Ciências, Lisbon, Portugal, <sup>bb</sup>University of California at Irvine, Irvine,

USA, <sup>cc</sup>University of Victoria, Victoria, Canada.

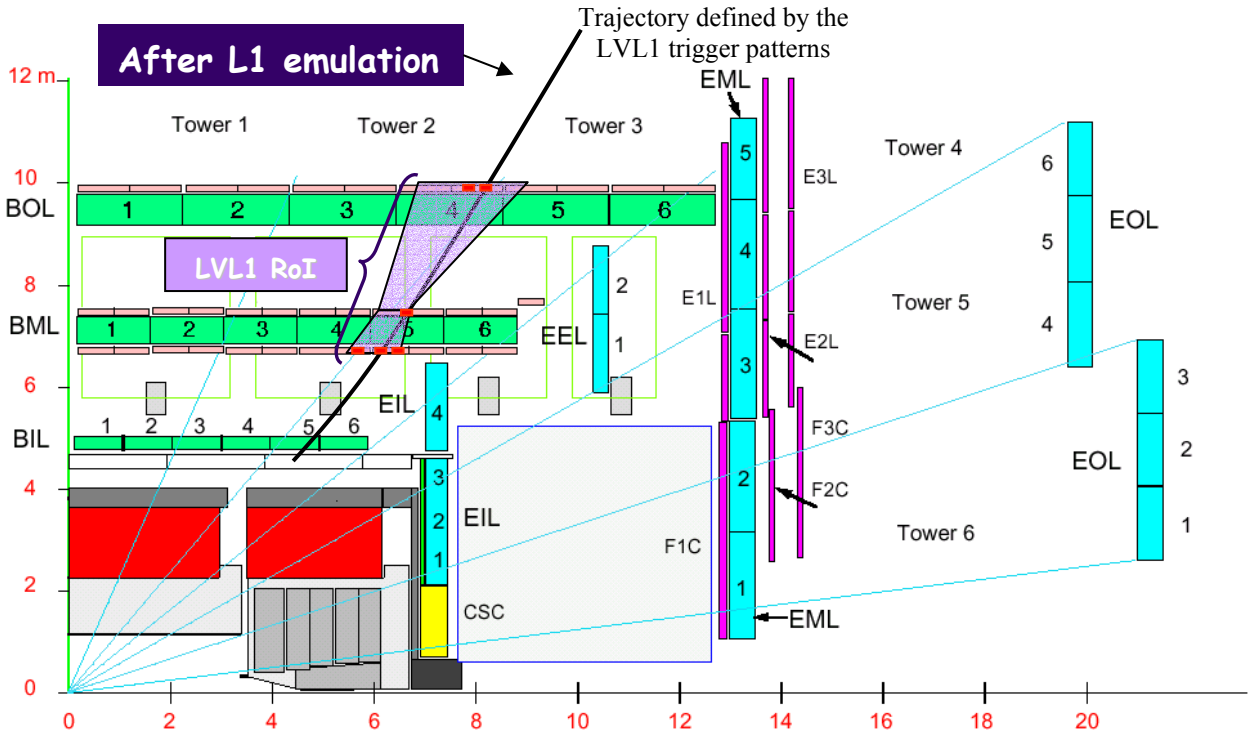


Figure 1: Longitudinal view of the ATLAS Muon Spectrometer showing the measurement stations for the barrel (BIL, BML, BOL) and for the endcap (EIL, EML, EOL). The Level-1 RoI for a muon track is also shown together with the hits left on trigger chamber (red dots) and the approximated trajectory reconstructed from RPC data.

planes of tracking chambers, arranged in three measurement stations (figure 1), which measure the coordinate in the bending projection with an intrinsic precision of  $80 \mu\text{m}$ . Monitored Drift Tubes (MDT) [2] technology is used in most of the Spectrometer. In the very forward region ( $2 \leq \eta \leq 3$ ) Cathode Strip Chambers (CSC) [2] are employed because they support a higher particle flux. The tracking system is complemented with an independent and fast trigger system that provides also the measurement of the second coordinate. The trigger system employs Resistive Plate Chambers (RPC) [3] in the barrel and Thin Gap Chambers (TGC) [4] in the endcaps.

## THE ATLAS TRIGGER

The ATLAS trigger performs the event selection in three sequential steps of increasing complexity: Level-1, Level-2 and Event Filter. The Level-1 trigger [5] receives the data at the bunch crossing frequency (40 MHz). The latency time is about  $2 \mu\text{s}$  and the maximum output rate is 75 KHz. The trigger is made of hardwired processors which analyze coarse granularity data and apply simple algorithms to find physics activities above threshold. In the Muon System only data from trigger chambers are used to take a trigger decision.

The other two trigger levels [6] are based on software algorithms which run in processor farms. Level-2 uses the full granularity data but processes only the detector regions flagged by Level-1 as containing activity, the so called Regions of Interest (RoIs). This technique reduces

the data throughput down to 2% of the full event. The Level-2 analysis is performed in two steps: first fast algorithms reconstruct physics objects ( $e$ ,  $\gamma$ ,  $\mu$ , jets ...) within the RoIs, then the event is selected combining the physics objects according to a trigger menu. Altogether the Level-2 reduces the event rate by a factor of about 100 with a mean latency time of 10 ms.

The Event Filter is the last stage of the online selection and access the full event data. At this stage the latency time is  $\sim 2 \text{ s}$  and allows to use offline-like algorithms that provide a refined reconstruction of the physics objects. The Event Filter performs the final classification of the events reducing the event rate by a further factor of 10.

## LEVEL-2 MUON RECONSTRUCTION

Muon reconstruction at Level-2 is performed to confirm the Level-1 muon RoI and to build “muon” objects for the trigger menu. It proceeds through the “ $\mu\text{Fast}$ ” algorithm that, using only the Muon Spectrometer data, provides an accurate muon track reconstruction within an RoI and a precise estimation of the muon  $p_T$  at the interaction vertex. These parameters are subsequently refined using other detector data (Inner Detector to refine the  $p_T$  estimation, Calorimeters to provide isolation checks) by different algorithms.

$\mu\text{Fast}$  gathers together RoI data and processes them in three sequential steps:

- “Global Pattern Recognition” which involves trigger chambers data and positions of MDT tubes;

- “Track Fit” using the drift time measurements, performed on each MDT chamber;
- “Fast  $p_T$  Estimate” using a Look Up Table to avoid a time consuming fit method.

The result of the algorithm is the  $\eta$ ,  $\phi$  position and the direction of flight of the muon track, plus the muon  $p_T$  at vertex.

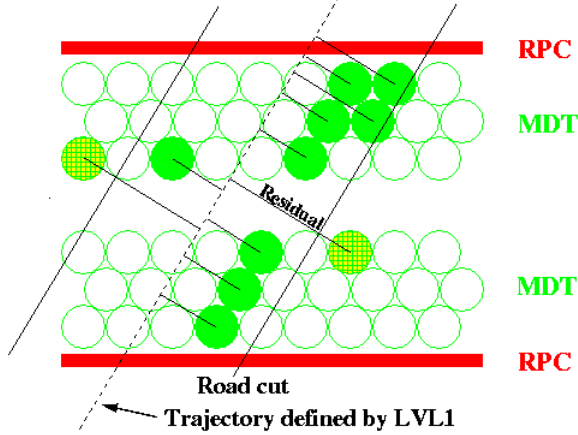


Figure 2: example of the MDT pattern recognition in a barrel middle station (BML). Residuals are the distance of the centre of hit tube from the Level-1 trajectory.

The global pattern recognition selects MDT muon hits for the track fit, and is seeded by the trigger chambers data. Trigger hits plus the interaction vertex position are used to define the initiator of the muon trajectory (figure 1), then a road is opened around this trajectory to collect MDT hit tubes within it (figure 2). A contiguity algorithm is finally applied on the selected hits to further remove the background. Notwithstanding the road dimension are very tight ( $\sim 20$  cm) this method selects muon hits with 96% of efficiency.

In order to save CPU time, the muon track is fitted locally on each MDT station through straight segments, using only 1 hit per MDT layer. The intersection of the fitted lines with the middle of the chamber determines precision points used to compute the track sagitta. For the fit, an approximated R-t relation is used (no Lorentz effects are taken into account) and the time-of-flight and propagation time along the wire are subtracted from the raw drift time. The approximations (use of straight segments instead of a curve and no use of the calibrated R-t relations) are negligible with respect to the muon sagitta for  $p_T$  equal to the trigger thresholds:  $\sim 5$  cm (20 GeV) and  $\sim 25$  cm (6 GeV).

Finally the muon transverse momentum is estimated using a linear relationship between the measured sagitta ( $s_m$ ) and  $p_T$

$$\frac{1}{s_m} = A_0 \cdot p_T + A_1$$

which is stored in Look Up Tables for different  $\eta$ ,  $\phi$  regions. To take into account the non-uniformity of the magnetic field, the energy loss of the muon when it crosses the calorimeters and the multiple scattering at the

calorimeters exit, tables with an  $\eta$ ,  $\phi$  granularity of  $30 \times 60$  are used for each detector octant. The total data volume of the LUTs is about 130 Kbytes.

### $\mu$ Fast performances

The aim of  $\mu$ Fast is to reject fake muons accepted by the Level-1 trigger, to perform a measurement of the transverse momentum of muon candidates, and to exclude those muon tracks with a momentum below threshold. The physics performance indicators are thus the track finding efficiency relative to the Level-1 output, and the resolution of the reconstructed muon  $p_T$ .

The track finding efficiency is determined by the hit selection efficiency of the muon roads and by the geometrical coverage of the MDT chambers. While the former is tunable, the latter contributes approximately to (1-3)% of the total inefficiency depending on the muon momentum. The net track finding efficiency of  $\mu$ Fast is about 97%.

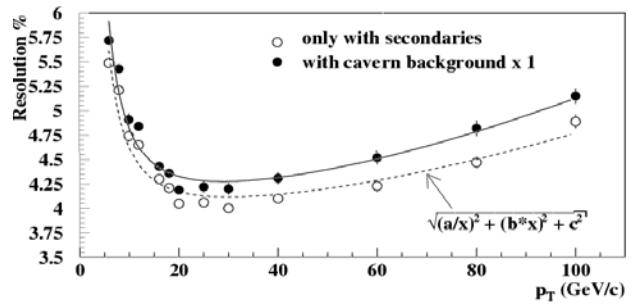


Figure 3: The  $p_T$  resolution of  $\mu$ Fast as a function of the muon  $p_T$  in the region  $|\eta| \leq 1$ . The Cavern Background is simulated at the maximum luminosity.

The  $p_T$  resolution of the algorithm has been measured with and without Cavern Background<sup>†</sup> (figure 3). The resolution is not significantly degraded by the presence of background and is about 6% for the 6 GeV threshold and 4% for the 20 GeV threshold. These values are only a factor of two worse than those obtained by the offline reconstruction program.

The algorithm is optimized to yield a trigger efficiency for prompt muons of 90% at threshold. The good resolution on transverse momentum allows to apply a  $p_T$  cut much sharper than the one applied by the Level-1, thus reducing the event rate of the non prompt muons coming from the  $\pi/k$  decays. This reduction is more effective at the low- $p_T$  threshold (6 GeV) where the  $\pi/k$  decays cross section dominates the inclusive muon production and is exponentially increasing towards  $p_T=0$ .

A summary of the muon event rates at Level-1 and at Level-2 using  $\mu$ Fast is shown in Table 1.  $\mu$ Fast reduces the total muon event rate by a factor of 2 at low- $p_T$  threshold and by a factor of 10 at high- $p_T$  threshold.

<sup>†</sup> Cavern Background is constituted by low energy neutrons and photons which originates from the collisions at the vertex. Hits from these particles are the dominant contribution to the difficulties of performing the pattern recognition.

Table 1: total output rates of the Level-1 and Level-2 muon trigger for the barrel region ( $|\eta| \leq 1$ ).

Processes	6 GeV ( $10^{33} \text{ cm}^{-2} \text{ s}^{-1}$ )		20 GeV ( $10^{34} \text{ cm}^{-2} \text{ s}^{-1}$ )	
	Level-1 KHz	$\mu$ Fast KHz	Level-1 KHz	$\mu$ Fast KHz
Beauty	1.40	0.75	0.50	0.06
Charm	0.80	0.40	0.21	0.02
$W \rightarrow \nu\mu$	0.003	0.003	0.03	0.02
$\pi/k$ decays	7.10	2.70	0.68	0.04
Fakes	1.0	$\sim 0$	$\sim 0$	$\sim 0$
Total	10.3	3.9	1.42	0.15

## CODE OPTIMIZATION

The  $\mu$ Fast code runs in the Level-2 processing unit (L2PU), the trigger component that steers the algorithms to classify the event and manages the RoI data requests. The target Level-2 mean event processing time is 10 ms, thus the fraction of processing time left to  $\mu$ Fast reconstruction is  $O(1 \text{ ms})^\ddagger$ .

To meet this strict constraint, the design of  $\mu$ Fast doesn't employ techniques that increase the CPU load, like memory allocation on demand or data organization through STL containers. The reconstruction tasks described in the previous section are implemented by procedures that operate on data organized in appropriate structures. This reduces at minimum the latency due to the exchange of complex classes modelling the data, and at the same time allows a fast access to the processed data.

Further optimization is achieved tuning the definition of the trajectory reconstructed from RPC data using the position of the interaction vertex. As a result the muon road size is reduced, becoming much smaller than the MDT chamber dimension, while the muon hit selection efficiency is left untouched. This simplifies the task of the pattern recognition yielding a reduction of the overall processing time. A small road size increases the algorithm robustness against background: it removes most of the MDT hits present in a chamber, that arise from background in the ATLAS cavern.

The optimization work has also concerned with the procedure for requesting the event data. Inside the L2PU,  $\mu$ Fast receives RoI data through an infrastructure which is implemented using offline software components. Such components access raw data from detector elements inside the RoI region and automatically convert them into data classes suitable for the reconstruction. Those components are not optimized for speed. Thus the data request competes with the algorithm processing in terms of CPU usage and dominates the overall processing time if it is not tuned for the muon case.

<sup>‡</sup>  $\mu$ Fast is not the only algorithm to run on muon events; the reconstruction of muon tracks is also performed in the Inner Detector and in the Calorimeters to refine the muon object properties.

In particular, accessing the MDT chambers data through the muon RoI region is not efficient: typically seven MDT chambers belong to a muon RoI, while the muon track data are inside three of them. On the contrary the muon road selects a thin slice of the Spectrometer around the muon track. So it is the best candidate for issuing the MDT data request because it eliminates the time overhead due to the conversion of useless data.

Though it is not allowed to modify the infrastructure that converts the raw data, optimization is still possible by choosing a data model structure that eases the decoding task and thus saves processing time. Further optimization in this area is obtained performing the "data preparation" (i.e. associate space points to detector hits, calibrate the data, ...) only on the data entering the fit. This implies to perform this task inside the algorithm employing an ad hoc code that provides fast access to the detector geometry.

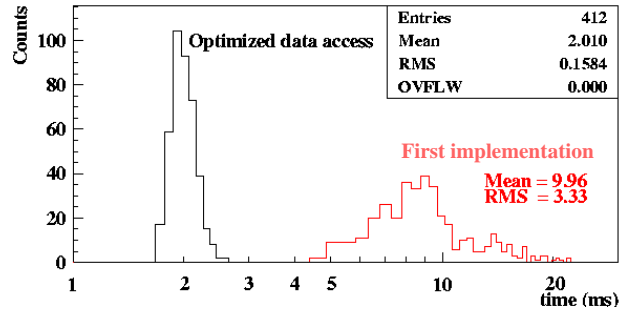


Figure 4: Execution time of the Level-2 muon reconstruction on a XEON CPU clocked at 2.4 GHz.

The result of this optimization work is shown in figure 4, where the execution time of an old  $\mu$ Fast implementation is matched with the optimized one. The optimized version is fully compliant with the Level-2 latency.

## REFERENCES

- [1] ATLAS Technical Proposal for a General-Purpose pp Experiment at the Large Hadron Collider at CERN, CERN/LHCC/94-43, LHCC/P2, 15 December 1994.
- [2] ATLAS Muon Spectrometer Technical Design Report, CERN/LHCC/97-22, 31 May 1997.
- [3] Rinaldo Santonico, "Topics in resistive plate chambers and related detectors; Università di Pavia, 1996.
- [4] Y. Ari et al., "Thin Gap Chamber: Performances as a Time and Position Measuring Device", SCIENTIFICA ACTA: Resistive plate chambers and related detectors; Università di Pavia, 1996.
- [5] ATLAS Level-1 Trigger Technical Design Report, CERN/LHCC/98-14, 24 June 1998.
- [6] ATLAS High-Level Trigger Data Acquisition and Controls Technical Design Report, CERN/LHCC/2003-022, 30 June 2003.